
Article:
Aldemir Dikici, B., Malayeri, A., Sherborne, C. et al. (9 more authors) (2022) Thiolene- and polycaprolactone methacrylate-based polymerized high internal phase emulsion (PolyHIPE) scaffolds for tissue engineering. Biomacromolecules, 23 (3). pp. 720-730. ISSN 1525-7797

https://doi.org/10.1021/acs.biomac.1c01129

Thiolene and polycaprolactone methacrylate-based polymerised high internal phase emulsion (PolyHIPE) scaffolds for tissue engineering

Betül Aldemir Dikici [a, b, c], Atra Malayeri [a], Colin Sherborne [a], Serkan Dikici [a, c], Thomas Paterson [d], Lindsey Dew [a], Paul Hatton [d], Ilida Ortega Asencio [d], Sheila MacNeil [a], Caitlin Langford [e], Neil R. Cameron [f, g], Frederik Claeyssens [a, b] *

[a] Department of Materials Science and Engineering, University of Sheffield, Kroto Research Institute, Sheffield, S3 7HQ, United Kingdom

[b] Department of Materials Science and Engineering, INSIGNEO Institute for In Silico Medicine, University of Sheffield, The Pam Liversidge Building, Sheffield, S1 3JD, United Kingdom

[c] Department of Bioengineering, Izmir Institute of Technology, Urla, Izmir, 35433, Turkey

[d] School of Clinical Dentistry, University of Sheffield, Sheffield, S10 2TA, United Kingdom

[e] Perspectum Diagnostics, Oxford, OX4 2LL, United Kingdom

[f] Department of Materials Science and Engineering, Monash University, 22 Alliance Lane, Clayton, VIC 3800, Australia

[g] School of Engineering, University of Warwick, Coventry CV4 7AL, United Kingdom

***Corresponding author:** *f.claeyssens@sheffield.ac.uk*

Abstract:

Highly porous emulsion templated polymers (PolyHIPEs) provide a number of potential advantages in the fabrication of scaffolds for tissue engineering and regenerative medicine. Porosity enables cell ingrowth and nutrient diffusion within - as well as waste removal from - the scaffold. The properties offered by emulsion templating alone include the provision of high interconnected porosity, and - in combination with additive manufacturing – the opportunity to introduce controlled multi-scale porosity to complex or custom structures. However, the majority of monomer systems reported for PolyHIPE preparation are unsuitable for clinical applications as they are non-degradable. Thiol-ene chemistry is a promising route to produce biodegradable photocurable PolyHIPEs for the fabrication of scaffolds using conventional or additive manufacturing methods, however, relatively little research has been reported on this approach. This study reports the groundwork to fabricate a thiol and polycaprolactone (PCL) based PolyHIPE materials via a photoinitiated thiolene click reaction. Two different formulations, either 3-arm PCL methacrylate (3PCLMA) or 4-arm PCL methacrylate (4PCLMA) moieties were used in the PolyHIPE formulation. Biocompatibility of the PolyHIPEs was investigated using human dermal fibroblasts (HDFs) and human osteosarcoma cell line (MG-63) by DNA quantification assay, and developed PolyHIPEs were shown to be capable of supporting cell attachment and viability.

Keywords: *emulsion templating*, *PolyHIPE, polycaprolactone, thiol-ene, tissue engineering, biomaterials, photopolymerisation, porosity*

1. Introduction

A key aspect when producing scaffolds for biomedical applications is the inclusion of interconnected porosity within the construct; this enables cell ingrowth, nutrient diffusion and waste removal from the implanted scaffold. Various methods reported to fabricate porous substrates for biomedical applications include electrospinning [1–3], 3D printing [4], and porogen leaching [5,6]. Emulsion templating is an alternative fabrication route that has gained attention due to its advantages of being (i) tunable, (ii) providing high porosity (up to 99%) and (iii) interconnectivity (open cellular morphology) [7]. While an interconnected porous scaffold is important for cell infiltration, tunable chemical, mechanical and morphological cues enable precise engineering of the substrates for specific biomedical applications. The principle of emulsion templating is based on creating biphasic emulsions and polymerisation of the continuous phase (Figure 1). Solidifying of a monomeric continuous phase and subsequent removal of the internal droplet phase leaves behind a porous structure that is a 3D replica of the initial emulsion. Emulsions with an internal volume higher than 74% are defined as **H**igh **I**nternal **P**hase **E**mulsions (**HIPEs**), and substrates obtained by their polymerisation are called **Poly**merised **HIPEs** (**PolyHIPEs**). To date, there has been a number of significant reviews from the pioneers of the field of emulsion templating in the literature [8–13]. Also, recently, comprehensive reviews on the development and use of PolyHIPEs specifically in biomedical applications has been reported [7,14].

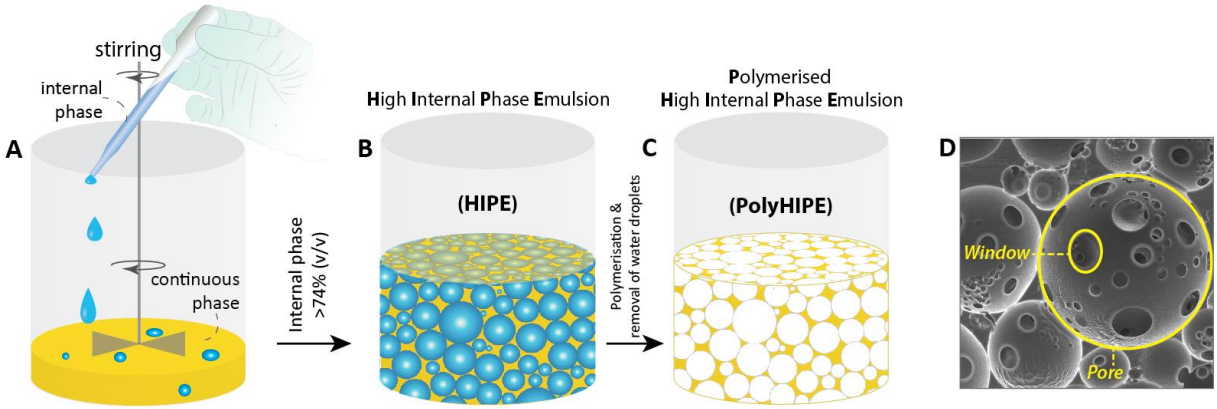

Figure 1: *Fabrication steps of the Polymerised High Internal Phase Emulsion (PolyHIPE). (A, B) The gradual addition of the internal phase into the continuous phase while the system is mixed, (C) polymerisation of the high internal phase emulsion (HIPE), (D) scanning electron microscope image of the PolyHIPE (Adapted from [7]).*

Common monomers reported in PolyHIPE preparations are styrene, its derivatives such as divinyl benzene (DVB) and acrylate-based monomers, including 2-ethyl-hexyl acrylate (EHA) and isobornyl acrylate (IBOA) [15–20]. The aforementioned conventional monomers have limited applications for tissue engineering as they do not degrade within the body.

To create a PolyHIPE scaffold often free radical initiated thermal polymerisation is used to set the monomeric continuous phase into a solid. However, the number of researchers using photopolymerisation to fabricate PolyHIPE scaffolds has increased [4,15–17,21–28]. Photocuring to produce PolyHIPEs is a fast and versatile approach; it allows a wide choice of monomers and permits the curing of less stable emulsions which would otherwise destabilise over the long thermal cure process [22].

There has been an emerging research effort exploring thiol-ene chemistry to produce biodegradable photocurable PolyHIPEs for tissue engineering applications [26,29,30]. The resulting PolyHIPE material formed via this chemistry is intended to be fully biodegradable as they are aliphatic polyesters. Caldwell et al. used a 1:1 trimethylolpropane tris (3-mercaptopropionate) (tri-thiol) and trimethylolpropane triacrylate (TMPTA) mixture to produce the degradable material [26]. Johnson et al. showed successful preparation of thiol and triacrylate polycaprolactone (PCL) based PolyHIPE by thiol-ene click chemistry, which resulted in a fully degradable PolyHIPE material (90% and 95% nominal porosity) with 60 µm void diameter [30]. Additionally, Susec et al. reported a biocompatible divinyl adipate and pentaerythritol tetrakis (3-mercaptopropionate) based PolyHIPEs, which they used in a follow-up study as scaffolds for cartilage repair [21,31]. Recently, Whitely et al. reported on the use of thiol additives (5-10%) to reduce the oxygen quenching of the radical initiated polymerisation with negligible change in the properties of the material and biocompatibility of their PolyHIPEs [32]. Additionally, Langford et al. have shown that thiol-ene based polyHIPEs can be consecutively functionalised via using the pendant sulphur groups as binding sites via click-chemistry [33].

To summarise, PolyHIPEs have tremendous potential as a scaffold fabrication approach to produce highly porous biomaterials, where controlled porosity may influence both mass transfer and cell attachment/migration. However, relatively little progress has been reported in the development of methods that are ideally suited to the preparation of biocompatible, biodegradable PolyHIPEs with properties tailored to tissue engineering. PCL has been widely reported as ideally suited for these applications on account of its excellent biocompatibility and favourable cell response [24,34,35], and the aim of this research was, therefore, to investigate a method to prepare thiolene and PCL methacrylate-based PolyHIPE scaffolds, and evaluate their *in vitro* biocompatibility.

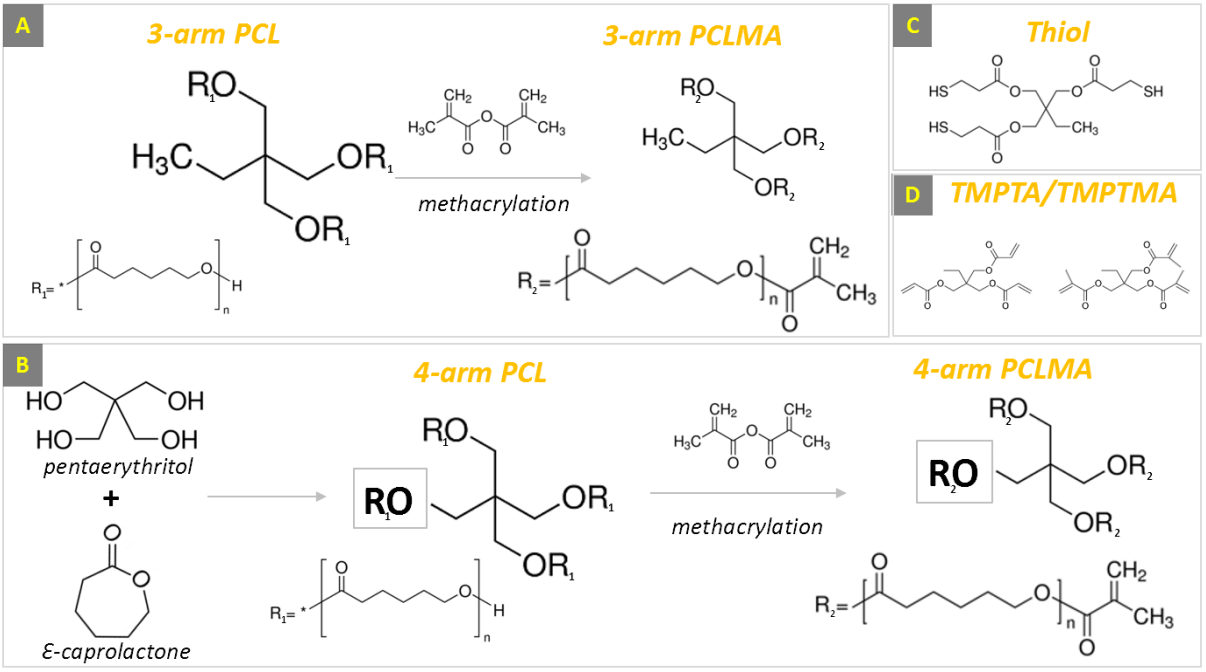

Figure 2: *Monomers used in the composition of Thiol-PCL PolyHIPEs. (A) Methacrylate functionalisation of PCL triol to obtain 3PCLMA, (B) Synthesis of 4PCL from ring-opening polymerisation of pentaerythritol and caprolactone and methacrylate functionalisation. Chemical structures of (C) tri-trithiol and (D) crosslinkers; TMPTA/TMPTMA.*

2. Materials and Methods

2.1. Materials

ε-Caprolactone, pentaerythritol, methacrylic anhydride (MAAn), chloroform, toluene, tin 2-ethylhexanoate ($SnOct_2$), dichloromethane (DCM), triethylamine (TEA) isopropanol, trimethylolpropane tris (3-mercaptopropionate) (thiol), trimethylolpropane triacrylate (TMPTA), trimethylolpropane trimethacrylate (TMPTMA), diphenyl (2,4,6-trimethyl benzoyl) phosphine oxide/2-hydroxy-2-methylpropiophenone blend (photoinitiator), 1,2-Dichloroethane (DCE), polycaprolactone triol (M_n 900 g/mol), Dulbecco's Modified Eagle Media (DMEM), amphotericin B, fetal calf serum (FCS), penicillin/streptomycin (PS), L-glutamine, trypsin, paraformaldehyde, resazurin sodium salt, MTT, ethanol, DAPI and Phalloidin were all purchased from Sigma Aldrich. Hypermer B246 (surfactant) was donated by Croda Ltd.

2.2. Synthesis of 3PCLMA

The PCL triol was methacrylate functionalised to obtain 3PCLMA (Figure 2A). First, PCL triol (M_n 900 g/mol, 1 molar equivalent) was dissolved in DCM. TEA (6 molar equivalent) was dissolved in 50 mL DCM was added to the solution. The mixture was cooled by submerging in a salted ice bath for

30 minutes. MAAn (6 molar equivalent) was dissolved in 50 mL DCM and was added dropwise using a dropping funnel. When MAAn was completely dispensed, the solution was allowed to warm up slowly to room temperature (RT) and was left to react for 24 hours while covered in foil. Almost all solvent was removed using a rotary evaporator, and the polymer was purified three times by precipitation from methanol at -80°C.

2.3. Synthesis of 4PCLMA

The synthesis of 4PCLMA was described in detail in other studies [2,23,24,36,37]. Briefly, 4PCL was synthesised via ring-opening polymerisation of ε-caprolactone and multifunctional alcohol initiator pentaerythritol and then methacrylate functionalised. 4PCLMA and pentaerythritol were then added to a round bottom flask in the presence of toluene stirred using a magnetic stirrer under a nitrogen atmosphere. The resulting reaction mixture was heated to 130°C, and $SnOct_2$ was added. Furthermore, the reaction was stirred continuously for 6 hours at RT prior to solvent removal via rotary evaporation. For the methacrylation, hydroxyl-terminated PCL was dissolved in DCM, then the solution was cooled in an ice bath before the addition of TEA (2 molar equivalents). MAAn (2 molar equivalents) was added dropwise whilst maintaining a low temperature. The reaction was allowed to stir for 24 hours at RT in the absence of light under nitrogen gas. Finally, the solvent was removed by rotary evaporation, and the polymer was purified three times by precipitation from methanol at -80°C.

2.3. Characterisation of 3PCLMA, 4PCL and 4PCLMA

Proton (^{1}H) nuclear magnetic resonance NMR spectroscopy analysis was performed on an AVANCE III spectrometer at 400 MHz to confirm the structure of 3PCLMA and 4PCLMA. The spectra were recorded using an 8.2 kHz acquisition window, with 64 k data points in 16 transients with a 60 s recycle delay (to ensure full relaxation). Deuterated chloroform was used as a diluent ($CDCl_3$). Spectra were analysed using MestReNova software. Chemical shifts were referenced relative to $CDCl_3$ at 7.27 ppm. The degree of methacrylation (DM) of 3PCLMA and 4PCLMA was calculated by comparing the signal intensity of the methylene groups and the signal intensities of the methacrylate groups from the NMR data (Equation 1, 2).

$$\boldsymbol{DM} = ((\int \boldsymbol{methacrylated\ ends})/(\int \boldsymbol{non-methacrylated} + \boldsymbol{methacrylated\ ends})) * \mathbf{100} \quad \textbf{(1)}$$

$$\boldsymbol{DM} = \frac{\left((\int \boldsymbol{I_{5.5}} + \int \boldsymbol{I_{6.1}})/\mathbf{2}\right)}{\left((\int \boldsymbol{I_{5.5}} + \int \boldsymbol{I_{6.1}})/\mathbf{2}\right) + \left((\int \boldsymbol{I_{3.6}})/\mathbf{2}\right)} \boldsymbol{x}\mathbf{100} \quad \textbf{(2)}$$

Molecular weight and molecular weight distributions of 4PCLMA were determined using a Viscotek GPCmax VE200 gel permeation chromatography (GPC) system with a differential refractive index detector (Waters 410). Tetrahydrofuran was used as the eluting solvent at a flow rate of 1 mL/minute at 40 °C, and polystyrene standards were used as the calibration sample.

2.6. Mechanical Characterisation 3PCLMA and 4PCLMA

Dog-bone shaped tensile test samples were fabricated as previously described [23] and mechanical test was applied as described previously [38]. Briefly, 0.5 mL 4PCLMA and 3PCLMA were pipetted into the moulds and cured for 3 min on each side. Samples were tested using a uniaxial mechanical testing machine (BOSE Electroforce Test Instruments, Minnesota, USA) equipped with a 22 N load cell. Grip distance and extension rate were set to 10 mm and 0.1 mm/s, respectively, and the force and elongation data were recorded. The stress and strain values were calculated using the cross-sectional area where force was applied. Young's modulus was determined using the linear-elastic region of each sample's stress-strain curves. The ultimate tensile strength (UTS) was calculated as that of the maximum force applied divided by the cross-sectional area of the sample.

2.4. Preparation of PolyHIPE Scaffolds

Thiol-PCL PolyHIPEs were manufactured via photopolymerisation with the formulations presented in Figure 5A. The continuous phase of the emulsion consisted of PCL, thiol, surfactant (Hypermer B246), and crosslinker were dissolved in the solvent and stirred using an overhead stirrer (Pro40, SciQuip). The water was added dropwise, and then the emulsion was left to further mix for a further 5 minutes. Finally, the photoinitiator was added in the absence of light, mixed and transferred to a silicone mould and cured via Light Hammer® 6 UV curing system (Fusion UV Systems Inc, USA) assisted with bench-top conveyor (LC6E, Fusion UV Systems Inc, USA) with a power output of 200 W/cm^2 at 100% intensity.

PCL-Thiol PolyHIPE samples were washed in a Soxhlet extractor for 24 hours with ethanol. For cell culture, the samples were transferred to a 70% ethanol and distilled water solution for 30 minutes. The samples were transferred to sterile PBS and washed three times to remove traces of ethanol. To remove all trapped air from the discs, the samples were kept in a sterile PBS container, a lid affixed with a 0.2 µm pore syringe filter was used to seal the container, which was then put into a vacuum oven and cycled from being under vacuum to normal atmospheric pressure to draw the trapped air out of the sample. This was repeated three times until all the samples remained submerged under normal atmospheric pressure.

2.5. Chemical and Morphological Characterisation of PolyHIPEs

To prepare the 4PCLMA and 3PCLMA based PolyHIPE specimens for SEM they were first freeze-dried and cut to reveal their internal cross-section. These were then attached to carbon fibre pads adhered to aluminium stubs and sputter-coated with gold (Emscope SC500, Philips). The morphologies of the PolyHIPE disks were then imaged using a Philips XL-20 scanning electron microscope operating at 10.0 kV. The SEM micrographs were analysed using the software Image J 1.48 to quantify the average void diameter of PolyHIPE disks, the diameters of 90 voids and 20 windows were measured, and a statistical correction factor was applied to the average void diameter [39]. Pore and window size distribution histograms were created and average pore (D) and window sizes (d) were reported. The degree of interconnectivity was calculated by dividing the average window size by the average pore size (d/D) [23,40], and the degree of openness was calculated by dividing open surface area by total surface area for randomly selected 10 pores [7,13,17]. Fourier Transform Infrared spectroscopy was performed on Thiolene 4PCLMA PolyHIPE. Readings were taken between 500 – 4000 cm^{-1} and resolution of 4 cm^{-1}.

2.5. Biological Characterisation

2.5.1. Fibroblast Cell Culture

Human dermal fibroblast cells were isolated from tissue samples obtained from consenting patients undergoing either elective abdominoplasty or breast reduction surgery as described previously [3,23,41]. The collected tissue was used under the requirements stipulated by the Research Tissue Bank Licence 12179, and fibroblast cells were isolated (Ethical approval for the tissue acquisition was granted by the local ethical approval committee of the NHS Trust, Sheffield, UK, ethics reference: 15/YH/0177). The fibroblasts were cultured and expanded in T75 culture flasks until they were ~80% confluent. Scaffolds were disinfected in ethanol and washed with PBS three times. Dulbecco's modified Eagle's medium supplemented with 10% FCS, 0.01% L-Glutamine, 0.01% penicillin-streptomycin and 0.0025% amphotericin B was used as cell culture media. Cells were trypsinised and were seeded with the concentration of 75000 cells/40 µL media and were left in the incubator at 37°C, 5% CO_2 for 20 minutes for cell attachment before 1 mL of media was added. The cell medium was changed every three days.

2.5.2. Bone Cell Culture

The manufactured PolyHIPE disks had a diameter of 9 mm, which were washed in acetone and air-dried prior to the sterilisation process. The PolyHIPE disks were sterilised by immersing in 70% ethanol for 50 minutes following series of PBS washes (5 minutes, repeated three times). PolyHIPE disks were then air-dried in a sterilised environment for 48 hours prior to DMEM media soaking for 24 hours.

Human osteosarcoma cell line (MG-63) was used to seed disks with the density of 20000 cells (10 µL) per sample and placed in an incubator (37°C and 5% CO_2) for 30 minutes before addition of 990 µL of cell culture medium and tissue culture plastic was used as control. The samples were left in the incubator for a period of 3 and 7 days, and the medium was changed every two days.

2.5.3. Colourimetric Assays

Resazurin reduction (RR) assay was applied to measure the cellular metabolic activity and estimate the cell viability on scaffolds. Resazurin solution (non-fluorescent, blue) is reduced by the cells and forms resorufin (fluorescent, pink), which is detectable by a fluorescence plate reader. 1 mM resazurin stock solution in dH_2O was diluted to 100 µM in culture media to make the resazurin working solution. 1 mL of RR solution was added to each well, and the scaffolds were transferred into a fresh well plate using sterile forceps. The well plates were protected from light and incubated for 4 hours at 37 °C. From each scaffold, triplicate samples of 200 µL of the reduced solution were added to a 96 well plate. It was measured three times using a spectrofluorometer (FLX800, BIO-TEK Instruments, Inc.) at an excitation wavelength of 540 nm and an emission wavelength of 630 nm. Scaffolds were washed twice with PBS before adding fresh media. RR assay was performed at three time points (day 1, day 4, and day 7) with fresh scaffold/cell constructs for each. The reaction of blank (cell-free) PolyHIPEs with MTT reagent was also investigated. For this, first, 1 mg/mL MTT solution was prepared in PBS and filter sterilised. Scaffolds were placed into a fresh 24-well plate, and 1 mL of MTT reagent was added into each well, covered aluminium foil and incubated for 4 hours and 24 hours at 37°C. Colour change due to formed formazan crystals was imaged.

2.5.3. DNA Quantification Assay

Quant-iT^{TM} PicoGreen dsDNA Assay kit (Life Technologies, UK) is a DNA quantitation assay used to determine the cell number. Cell culture medium was removed from samples following series of PBS washes prior to treatment with 500 µL cell assay buffer (1:10 Tris-EDTA (TE) buffer (1.5 M Tris-HCL, 1 mM $ZnCl_2$, 1 mM $MgCl_2$) in deionised water and 1% Triton-X100) for each time point at room temperature for 30 minutes following overnight freeze at 4°C. The samples were treated through a series of freeze-thaw cycles, freeze (-80°C, 10 minutes) and thaw (37°C, 15 minutes) repeated three times. Following 15 seconds of vortexing and they were centrifuged at 10000 rpm for 5 minutes. 180 µL of supernatant was added in 1:1 ratio to PicoGreen reagent (diluted in 1:20 TE buffer (10 mM Tris-HCL, 1 mM EDTA, pH 7.5), 1:200 PicoGreen in deionised water). The samples were incubated at room temperature for 10 minutes in darkness prior to fluorescence reading at λ_{ex} = 485 nm and λ_{em} = 528 nm.

2.5.2. Confocal Microscopy

4',6-diamidino-2-phenylindole (DAPI) and TRITC-phalloidin stained specimens were prepared by diluting the stains (1:1000 in PBS) and incubated at room temperature for 30 minutes in darkness as described previously [15,17,42]. Single plane images (1024×1024 pixels) were taken via an upright confocal microscope (Zeiss LSM510-META, UK) assisted with ×10 objective (W-N-Achroplan 10×/N.A. 0.3, Zeiss ltd, UK). DAPI stain was excited using an 800 nm two-photon Ti-Sapphire laser set to 358 nm λ_{ex}, 461 nm λ_{em}. TRITC and FITC phalloidin (F-actin) was determined via single-photon laser set to λ_{ex} = 495 nm, λ_{em} = 515 nm (FITC) and λ_{ex} = 545 nm, λ_{em} = 573 nm (TRITC).

2.6. Statistical Analysis

Statistical analyses were performed by using GraphPad Prism 6 using one-way and two-way analysis of variance (ANOVA) for mechanical testing and cellular metabolic activity assays, respectively, and plotted as mean ± SD. A difference was deemed statistically significant if the p-value was less than 0.05, and the statistical differences are denoted in the figures. The total numbers of replicates (n) are stated in the figure legends.

3. Results and Discussion

3.1. Synthesis and the characterisation of 3PCLMA and 4PCLMA

PCL is one of the most widely used synthetic polymers used to fabricate tissue engineering scaffolds. Yet, its potential is limited by its form. Typically, PCL is a thermoplastic that is sold as small solid beads of various high molecular weights (60.000-90.000 g/mol), these can be dissolved in a solvent and electrospun into a fibrous scaffold, cast into a porous material by porogen leaching, or melted and extruded into the desired shape [35,43–45]. Photocurable monomers have gained increasing attention because of their potential to rapidly polymerise (seconds to minutes depending on the sample size) and their suitability to be used with a variety of fabrication techniques which include 3D printing [4,46,47], porogen leaching [48], and emulsion templating [2,23,24]. There is a limited range of commercially available degradable monomers. So, *in house* synthesis of photocurable monomers are often used. Functionalised 2-arm [49–51], 3-arm [30,52] and 4-arm [2,4,23,24] PCLs are forms of PCL used for tissue engineering applications. The molecular weight of the polymer [53] it's degree of functionalization [46] and the number of monomer arms [53] have been shown to influence the mechanical properties of these polymers. This photo-polymerisation of PCL expands the potential of this material to a range of tissue engineering applications. The FDA approval of PCL made medical devices on the market is encouraging for PCL to be used for other biomedical applications [23,54]. With similar motivation, there has been a

number of studies in the literature on the development of PCL based PolyHIPE structures either using radical polymerization or ring-opening polymerization [23,30,55–62].

In this study, the synthesis of 4PCL and methacrylate-functionalisation of both synthesised 4PCL and commercially available 3PCL is presented. 3PCL and 4PCL were successfully functionalised via methacrylate functionalisation. According to ^{1}H NMR analysis (Figure 3), while the non-methacrylated end of 3PCL and 4PCL has methylene groups adjacent to hydroxyl end groups shown with the peak at 3.6 ppm. On the methacrylated ends, they are converted into methacrylate groups, which are indicated at peaks 1.9, 5.5 and 6.1 ppm. The degree of methacrylation of 3PCLMA and 4PCLMA was calculated as 44% and 46%, respectively. The degrees of methacrylation of both 3PCLMA and 4PCLMA can be controlled using various parameters such as the ratio of methacrylation agents (methacrylic anhydride and triethylamine) to pre-polymer (PCL) and reaction time of methacrylation. Recently our group has reported the fabrication route of PCLMA with different degrees of methacrylation and the effect of methacrylation degree on mechanical properties of PCLMA [63]. In this study, we aimed to keep the degree of methacrylation constant for both types of polymer to compare their properties. But, the degree of methacrylation can be increased up to 100% for specific applications, such as bone tissue engineering scaffolds, as we reported before [4]. In this study, while PCL triol with a molecular weight of 900 g/mol was used for 3PCLMA, M_w and M_n values of 4PCLMA were determined by GPC analysis as 20900 g/mol and 15000 g/mol, respectively, which gives a dispersity of 1.4.

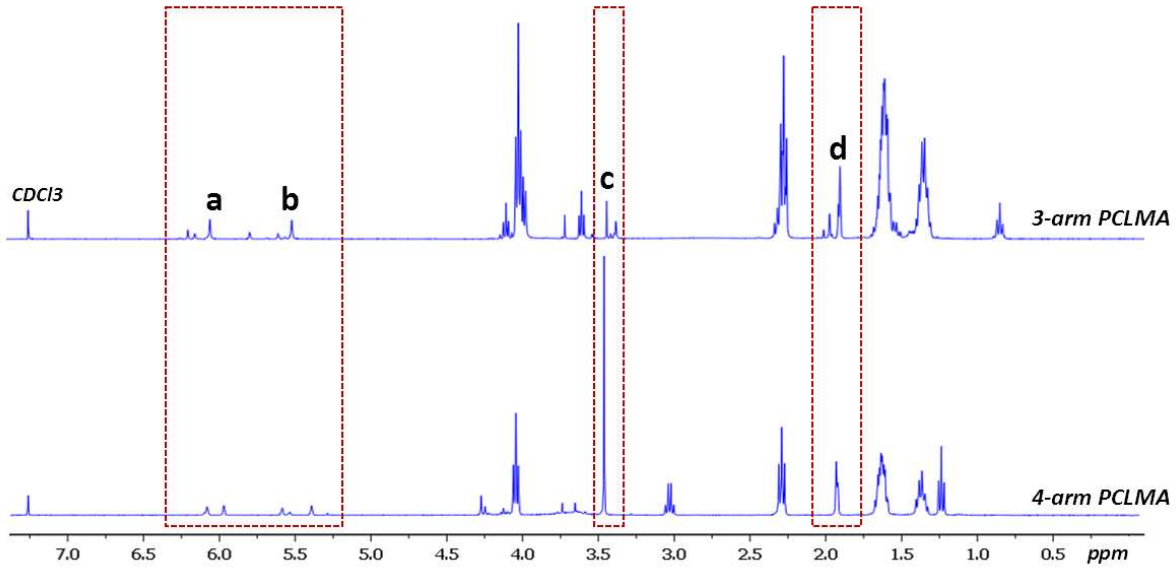

Figure 3: *Proton NMR spectrum of 3PCLMA and 4PCLMA and the relative assignments. c: the peaks of the hydroxyl group; a, b, and d are the peaks of the methacrylate group.*

Mechanical properties of the microenvironment are reported to have a dominant impact on cell behaviour. It is because cells can sense the stiffness of the material by mechanosensation and directs

its morphology, gene expression, and differentiation, accordingly [64–66]. Accordingly, we have investigated the mechanical properties of the polymer synthesized in the scope of this study; 3PCLMA and 4PCLMA. Tensile testing of 3PCLMA and 4PCLMA shows a significant difference between the mechanical properties of the two polymers. The 4PCLMA had the greater Young's modulus of 38.37±0.76 MPa and UTS of 3.20±0.10 MPa compared to the lower 3PCLMA values of 1.00±0.07 MPa and 0.25±0.04 MPa (Figure 4A, B). Digital images show the flexibility of 3PCLMA when compressed by fingers while the more rigid 4PCLMA resisted being bent (Figure 4C-F).

Overall; there are two main differences between the structural properties of 3PCLMA and 4PCLMA used in this study; (i) the number of branching (ii) the molecular weight. The main reasons for these 10-fold and 35-fold differences in UTS and Young's Modulus values of 3PCLMA and 4PCLMA are likely to be the difference in their crosslinking density and molecular weights (20-folds). 3CPLMA and 4PCLMA have a similar degree of functionalisation, but 4PCLMA has an additional branch, which will increase the crosslinking. Green et al. reported the UTS and tensile modulus of 79% acrylate-functionalised 3PCL (3PCLA, Mw: 900 g/mol) as 0.58±0.05 MPa and 4.0±0.5 MPa, respectively. This is also in line with the value reported by Field et al. of 3.51±0.5 MPa for 77% methacrylate functionalized 3PCL (3PCLMA, Mw 900 g/mol) [63]. Around 2 to the 4-fold difference between these mechanical properties is likely to be the difference in the degree of functionalisation.

It has been reported that an increasing number of arms enhance the mechanical properties of polymers [53,67]. Doganci et al. also, previously reported that three-armed star-shaped PCL has significantly lower elastic modulus due to high molecular chain mobility of 3-arm PCL compared to linear, four- and six-armed PCLs [68].

Secondly, an increase in the higher molecular weight of the polymers generally increases the mechanical strength of polymers and the glass transition temperature which has an impact on the storage modulus [69]. Tian et al. investigated the effects of molecular weight on properties of PCL networks and revealed that the length of the molecular chains directly influences the thermal and mechanical properties of the networks. Melting temperature (Tm), crystallinity, the crystallization temperature of the prepared PCL networks was shown to increase with increasing molecular weight. Also, polymers with higher molecular weight resulted in enhanced mechanical strength which was attributed to a higher degree of crystallization [70,71]. Similarly, Wang et al. reported the role of crystallinity on mechanical properties of photo-crosslinked poly(3-caprolactone fumarate) networks [72].

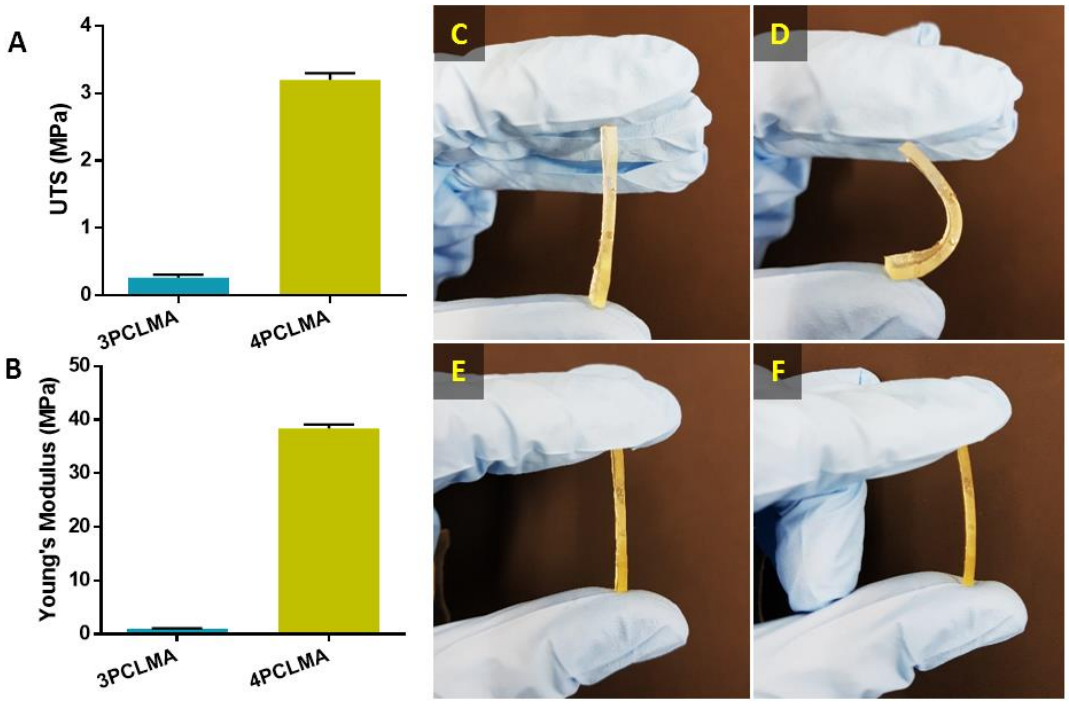

Figure 4: *(A) UTS, and (B) Young's Modulus values obtained from tensile testing of 3PCLMA and 4CLMA (mean ± STD error bars, n = 3). Digital photographs highlight the elastic properties of (C, D) 3PCLMA and (E, F) 4PCLMA before and during finger compression, respectively.*

3.2. Fabrication of PCLMA PolyHIPE Scaffolds

The emulsion ingredients and SEM pictures of the corresponding Thiol-3PCLMA and Thiol-4PCLMA PolyHIPEs are given in Figure 5A. The impact of solvent type and amount [23], water volume [17], emulsion temperature [73], and surfactant composition [74] on the morphology of the emulsion templated scaffolds has been previously reported. We intended to produce scaffolds with different pore sizes ranging from ten to a few hundred micrometres to show the tunability of this manufacturing method. Average pore sizes of thiol-3PCLMA PolyHIPE and thiol-4PCLMA PolyHIPE were calculated as 176.4±82.2 µm and 15.7±3.0 µm, respectively (Figure 5). Both of the formulations of PolyHIPE have shown open cellular morphology which is characterised by the presence of the windows between neighbouring pores (Figure 5B, C). The average window sizes were measured as 7.8±8.9 µm and 4.5±1.7 µm for the same groups, respectively. DOI and DOO values of thiol-4PCLMA PolyHIPE samples were calculated 7 and 3.6 fold higher than DOI and DOO values of thiol-3PCLMA PolyHIPEs. Although the number of pores was significantly higher in thiol-3PCLMA PolyHIPEs, as their relative window diameter (to the pore size) is smaller, it resulted in lower DOI and DOO in thiol-3PCLMA PolyHIPEs compared to thiol-4PCLMA PolyHIPE.

A

Group	PCL (g)	Trithiol (g)	Surf. (g)	Crosslinker (g)	Solvent (g)	PI (g)	H_2O (mL)	T (°C)	D [a] (µm)	d [b] (µm)	DOI [c]	DOO [d]	Porosity [e]	Density [f] (g/cm³)
3PCLMA	0.17	0.18	0.15	0.11 (TMPTA)	0.27 ($CHCl_3$)	0.03	4	60	176.4 ± 82.2	7.8 ± 8.9	0.04	0.07	87	0.14
4PCLMA	5.00	3.22	0.15	2.50 (TMPTMA)	11.25 (DCE)	0.56	35	23	15.7 ± 3.0	4.5 ± 1.7	0.28	0.25	77	0.26

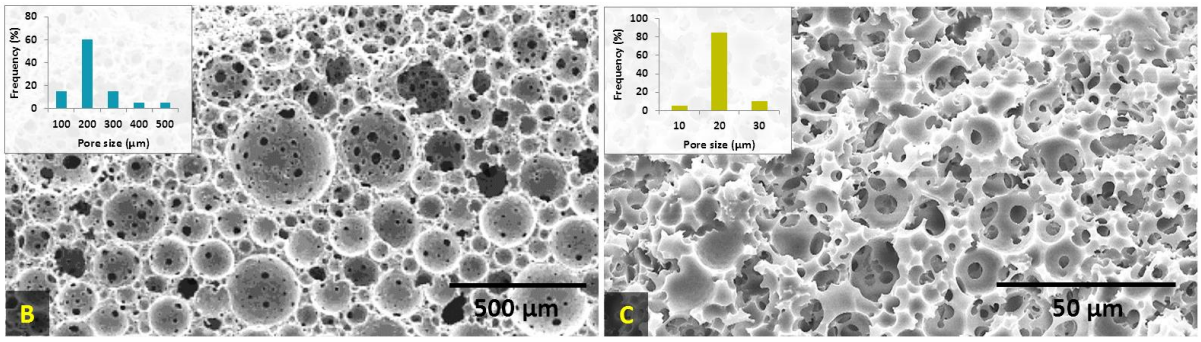

Figure 5: *(A) Composition, (B, C) Pore size distribution histograms and SEM micrographs of thiol-3PCLMA PolyHIPE and thiol-4PCLMA PolyHIPE, respectively. (a: average pore size, b: average window size, c: degree of interconnectivity, d: degree of openness, e: nominal porosity, f: expected density calculated based on porosity).*

As higher temperature also reduced the emulsion stability, the pore size distribution of 3PCLMA based PolyHIPE compared to the 4PCLMA was comparably wider (Figure 5B, C), which results in a significantly higher standard deviation than the average pore size seen in PolyHIPE scaffolds [26,40]. It is likely that the higher emulsion mixing temperature of 60°C is the main factor for the difference in the pore size between these samples as this reduces the emulsion stability, which causes more droplet coalescence and therefore larger pores. Also, there was a significant difference between the forms and viscosities of the polymers used in this study; while 3PCLMA was runny, liquid, 4PCLMA was solid at room temperature. This can be explained with ~20-folds molecular weight difference between 3PCLMA and 4PCLMA, as the viscosity of PCL is expected to increase with increasing molecular weight [45,75]. As the viscosity of the polymer directly affects the mixing efficiency of the two phases and emulsion formation, this may also contribute to a significant morphological difference between PolyHIPE groups. Additionally, the type of the diluting solvent used in the composition was reported to have an impact on the emulsion stability and average pore size of PolyHIPEs [23]. As chloroform has a higher density (1.480 g/mL) than DCE (1.256 g/mL), its use as a diluting solvent in the oil phase increases the density difference between the oil and water phase which increases the velocity of a single droplet in the emulsion according to Stoke`s Equation [7] and results in larger pore size.

3.3. Biological characterisation of PolyHIPE scaffolds

To assess the biocompatibility of the scaffolds, initially, an MTT assay was used. However, it was found that the scaffold alone also gave a positive signal from MTT (Figure 6). Also, Resazurin Reduction Assay

without any cells gave a false-positive result (Figure 6). MTT and RR assays are based on reduction of resazurin and MTT by reductase enzyme, present in mitochondria of metabolically active cells, into resorufin and formazan crystals, respectively. The initial blue and yellow colours are expected to turn to pink and black for MTT and RR, respectively.

FTIR spectrometry of the scaffolds shown free -SH groups on the polymer, which are likely the reducing agents for the metabolic dyes (small band between 685-690 cm^{-1} representing S-H band). So, the correlation of cell growth using their metabolic activity via MTT and RR is likely to provide spurious false-positive results. The fluorescence of the blanks samples should be measured and subtracted as a background absorbance to avoid overestimation of cell viability due to this noise [76]. Similarly, Langford et al. have shown the residual thiols of thiolene (meth)acrylate PolyHIPEs using Ellman's assay, which is a colourimetric assay [33].

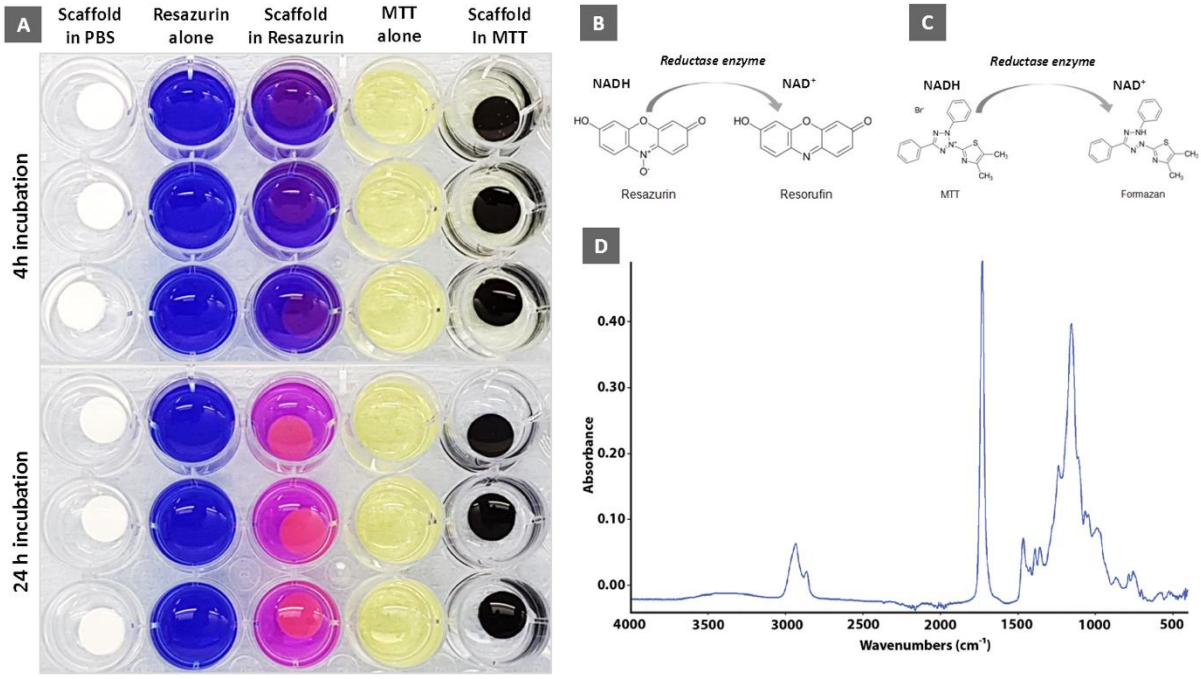

Figure 6: *(A) Testing the reaction of the scaffold (without any cells) itself with resazurin and MTT solutions. C/PBS: scaffold in PBS (control of scaffold), C/RR: resazurin solution alone (control of resazurin solution (RS)), S/RR: scaffold in RS (to test the reaction of the scaffold with RS), C/MTT: MTT solution alone (control of MTT solution), S/MTT: scaffold in MTT solution (to test the reaction of the scaffold with MTT solution), Incubation PCL Thiol PolyHIPE Discs in Resazurin Reduction and MTT solution. Working principles of (B) Resazurin Reduction assay and (C) MTT assay. (D) FTIR spectrum of PolyHIPE disks.*

In order to overcome the problem associated with MTT and RR assays being reduced by the polymer, PicoGreen DNA quantification assay was used to assess the DNA content of the samples to determine the biocompatibility of PolyHIPE scaffolds. According to Picogreen data, the cell viability of fibroblasts

shown an increasing trend from day three to day five on thiol-PCLMA PolyHIPEs (Figure 7A). A confocal image of seven days culture of fibroblast on flat sheets of thiol-3PCLMA polymer (not PolyHIPE) shows that cells attached, proliferated, and elongated on the polymer surface. Similarly, fibroblasts sit on the pores and spread over the walls of the PolyHIPE scaffold. Although polymer gives a blue background, Phalloiding TRITC staining clearly shown the cell cytoskeleton. Blue autofluorescence of thiol-PCL based PolyHIPEs also has been reported [30]. Similarly, the cell viability of MG63s on Thiol-4PCLMA PolyHIPE showed an increasing trend from day 3 to day 7. Seven days culture of MG63s were stained with both Phalloidin FITC and Phalloidin TRITC. Confocal images of both stainings show that cells elongated and spread over the pores of the PolyHIPE scaffold.

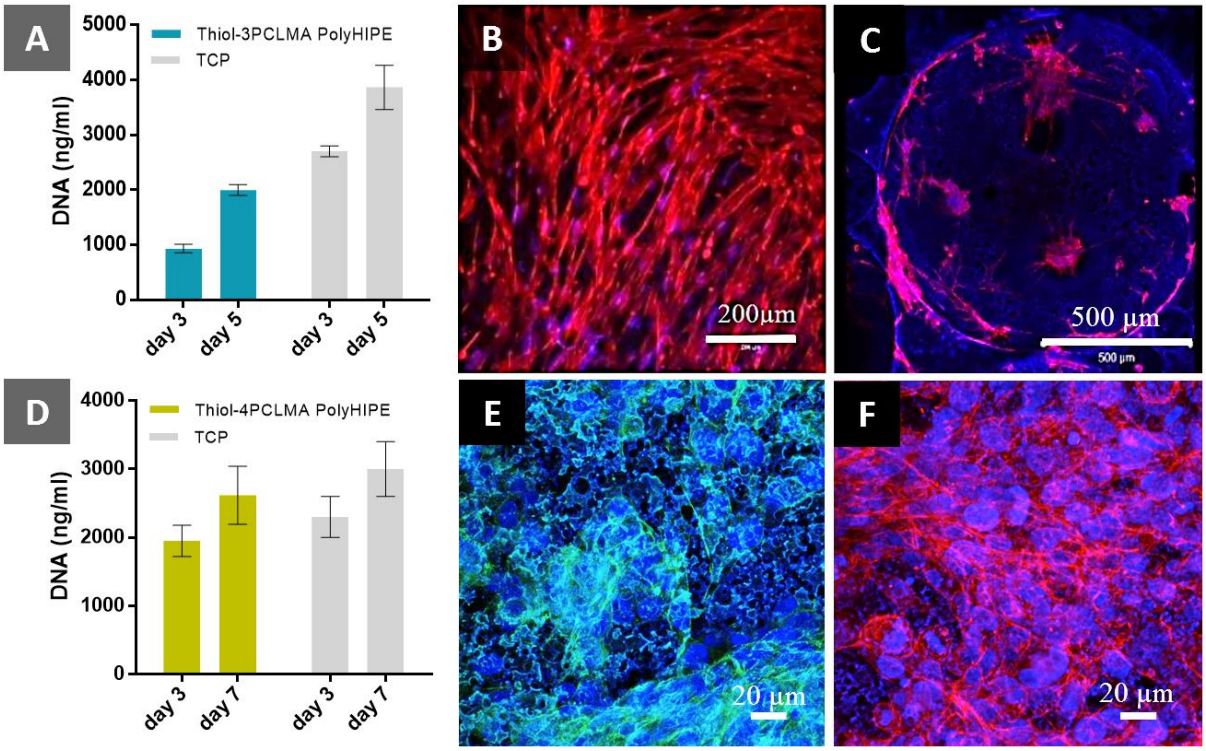

Figure 7: *(A) Cell viability of fibroblasts on thiol-3PCLMA PolyHIPE scaffolds (n=3). (B) Confocal image of 7-days culture of fibroblasts growing on thiol-3PCLMA. (C) Fluorescent confocal images of human dermal fibroblast cells growing on the PCL/Thiol PolyHIPE. (D) Cell viability of MG36s on thiol-4PCLMA PolyHIPE scaffolds (n=3). (E-F) Confocal image of 7-days culture of MG63s growing on thiol-4PCLMA. DAPI: blue, Phalloidin FITC: green, and Phalloidin TRITC: red.*

Previously Johnson et al. also reported the cell viability of L929 fibroblast on thiol-triacrylate functionalised PCL PolyHIPEs [30]. In this study, similar to our previous finding, cells tend to locate in the pores of PolyHIPEs with pore size larger than 20 µm, while they spread over the pores that have a diameter less than 20 µm [23]. Both 3PCLMA and 4PCLMA based thiolene PolyHIPEs have been shown to support cell attachment and cell viability.

4. Conclusion

In this study, thiol based PolyHIPEs using either 3PCLMA or 4PCLMA were fabricated successfully, and a tunability porosity was demonstrated. *In vitro* biocompatibility of PolyHIPEs was investigated using both HDFs and MG63 cells, and thiolene/acrylate-based PolyHIPEs were shown to provide a biocompatible substrate in terms of cell attachment and viability. In conclusion, this research demonstrated a route to synthesise novel Poly-HIPE PCL-based biomaterial that could be suitable for tissue engineering and regenerative medicine applications.

5. Acknowledgements

The authors gratefully acknowledge the Republic of Turkey – The Ministry of National Education for funding Betül Aldemir Dikici and Serkan Dikici. We acknowledge the Engineering and Physical Sciences Research Council (Grant No. EP/I007695/1) and the Medical Research Council (Grant No. MR/L012669/1) for funding the equipment used in this study. We are grateful to the UK Engineering and Physical Sciences Research Council (EPSRC) for supporting this work with a PhD studentship of AM with the "White Rose" DTC in Tissue Engineering & Regenerative Medicine (EP/L014823/1) and to The EPSRC Centre for Innovative Manufacturing in Medical Devices (MeDe Innovation, grant number EP/K029592/1). NC thanks to the Australian Research Council for support (DP190103309). We thank Dr Sandra van Meurs for her help on NMR analysis, interpretation, and calculation of the degree of functionalisation.

6. Author contributions

BAD contributed to the experimental design, analysis, data acquisition, and interpretation of data, statistical analysis, and drafting of the manuscript. AM contributed to the experimental design, analysis, data acquisition, interpretation of data and drafting of the manuscript. CS, SD, TP, and LD contributed to the experimental design, analysis, and data acquisition. CL and NC provided technical knowledge and equipment training. PH, IO, SM, NC, and FC contributed with their supervision and critical revision and editing of the manuscript.

References

(1) Mangir, N.; Aldemir Dikici, B.; Chapple, C. R.; MacNeil, S. Landmarks in Vaginal Mesh Development: Polypropylene Mesh for Treatment of SUI and POP. *Nat. Rev. Urol.* **2019**, *16* (11), 675–689. https://doi.org/10.1038/s41585-019-0230-2.

(2) Dikici, S.; Aldemir Dikici, B.; Bhaloo, S. I.; Balcells, M.; Edelman, E. R.; MacNeil, S.; Reilly, G. C.; Sherborne, C.; Claeyssens, F. Assessment of the Angiogenic Potential of 2-Deoxy-D-Ribose Using a Novel in Vitro 3D Dynamic Model in Comparison With Established in Vitro Assays. *Front. Bioeng. Biotechnol.* **2020**, *7* (451),

1–20. https://doi.org/10.3389/fbioe.2019.00451.

(3) Dikici, S.; Claeyssens, F.; MacNeil, S. Bioengineering Vascular Networks to Study Angiogenesis and Vascularization of Physiologically Relevant Tissue Models in Vitro. *ACS Biomater. Sci. Eng.* **2020**, *6* (6), 3513–3528. https://doi.org/10.1021/acsbiomaterials.0c00191.

(4) Aldemir Dikici, B.; Reilly, G. C.; Claeyssens, F. Boosting the Osteogenic and Angiogenic Performance of Multiscale Porous Polycaprolactone Scaffolds by in Vitro Generated Extracellular Matrix Decoration. *ACS Appl. Mater. Interfaces* **2020**, *12* (11), 12510–12524. https://doi.org/10.1021/acsami.9b23100.

(5) Thadavirul, N.; Pavasant, P.; Supaphol, P. Development of Polycaprolactone Porous Scaffolds by Combining Solvent Casting, Particulate Leaching, and Polymer Leaching Techniques for Bone Tissue Engineering. *J. Biomed. Mater. Res. Part A* **2014**, *102* (10), 3379–3392. https://doi.org/10.1002/jbm.a.35010.

(6) Owen, R.; Sherborne, C.; Evans, R.; C. Reilly, G.; Claeyssens, F. Combined Porogen Leaching and Emulsion Templating to Produce Bone Tissue Engineering Scaffolds. *Int. J. Bioprinting* **2020**, *6* (2), 99–113. https://doi.org/10.18063/ijb.v6i2.265.

(7) Aldemir Dikici, B.; Claeyssens, F. Basic Principles of Emulsion Templating and Its Use as an Emerging Manufacturing Method of Tissue Engineering Scaffolds. *Front. Bioeng. Biotechnol.* **2020**, *8* (875), 1–32. https://doi.org/10.3389/fbioe.2020.00875.

(8) Cameron, N. R. High Internal Phase Emulsion Templating as a Route to Well-Defined Porous Polymers. *Polymer (Guildf).* **2005**, *46* (5), 1439–1449. https://doi.org/10.1016/j.polymer.2004.11.097.

(9) Silverstein, M. S. PolyHIPEs: Recent Advances in Emulsion-Templated Porous Polymers. *Prog. Polym. Sci.* **2014**, *39* (1), 199–234. https://doi.org/10.1016/j.progpolymsci.2013.07.003.

(10) Silverstein, M. S. Emulsion-Templated Porous Polymers: A Retrospective Perspective. *Polymer (Guildf).* **2014**, *55* (1), 304–320. https://doi.org/10.1016/j.polymer.2013.08.068.

(11) Zhang, T.; Sanguramath, R. A.; Israel, S.; Silverstein, M. S. Emulsion Templating: Porous Polymers and Beyond. *Macromolecules* **2019**, *52* (15), 5445–5479. https://doi.org/10.1021/acs.macromol.8b02576.

(12) Silverstein, M. S.; Cameron, N. R. PolyHIPEs - Porous Polymers from High Internal Phase Emulsions. In *Encyclopedia of Polymer Science and Technology*; 2010. https://doi.org/10.1002/0471440264.pst571.

(13) Pulko, I.; Krajnc, P. High Internal Phase Emulsion Templating - A Path to Hierarchically Porous Functional Polymers. *Macromol. Rapid Commun.* **2012**, *33* (20), 1731–1746. https://doi.org/10.1002/marc.201200393.

(14) Kramer, S.; Cameron, N. R.; Krajnc, P. Porous Polymers from High Internal Phase Emulsions as Scaffolds for Biological Applications. *Polymers (Basel).* **2021**, *13* (11), 1786. https://doi.org/10.3390/polym13111786.

(15) Malayeri, A.; Sherborne, C.; Paterson, T.; Mittar, S.; Asencio, I. O.; Hatton, P. V.; Claeyssens, F. Osteosarcoma Growth on Trabecular Bone Mimicking Structures Manufactured via Laser Direct Write. *Int. J. Bioprinting* **2016**, *2* (2), 67–77. https://doi.org/10.18063/IJB.2016.02.005.

(16) Johnson, D. W.; Sherborne, C.; Didsbury, M. P.; Pateman, C.; Cameron, N. R.; Claeyssens, F. Macrostructuring of Emulsion-Templated Porous Polymers by 3D Laser Patterning. *Adv. Mater.* **2013**, *25* (23), 3178–3181. https://doi.org/10.1002/adma.201300552.

(17) Owen, R.; Sherborne, C.; Reilly, G. C.; Claeyssens, F.; Paterson, T.; Green, N. H.; Reilly, G. C.; Claeyssens, F. Emulsion Templated Scaffolds with Tunable Mechanical Properties for Bone Tissue Engineering. *J.*

Mech. Behav. Biomed. Mater. **2016**, *54* (2016), 159–172. https://doi.org/10.1016/j.jmbbm.2015.09.019.

(18) Gitli, T.; Silverstein, M. S. Bicontinuous Hydrogel–Hydrophobic Polymer Systems Through Emulsion Templated Simultaneous Polymerizations. *Soft Matter* **2008**, *4* (12), 2475. https://doi.org/10.1039/b809346f.

(19) Lépine, O.; Birot, M.; Deleuze, H. Preparation of a Poly(Furfuryl Alcohol)-Coated Highly Porous Polystyrene Matrix. *Macromol. Mater. Eng.* **2009**, *294* (9), 599–604. https://doi.org/10.1002/mame.200900102.

(20) Akay, G.; Birch, M. A.; Bokhari, M. A. Microcellular PolyHIPE Polymer Supports Osteoblast Growth and Bone Formation in Vitro. *Biomaterials* **2004**, *25* (18), 3991–4000. https://doi.org/10.1016/j.biomaterials.2003.10.086.

(21) Naranda, J.; Sušec, M.; Maver, U.; Gradišnik, L.; Gorenjak, M.; Vukasović, A.; Ivković, A.; Rupnik, M. S.; Vogrin, M.; Krajnc, P. Polyester Type PolyHIPE Scaffolds with an Interconnected Porous Structure for Cartilage Regeneration. *Sci. Rep.* **2016**, *6* (1), 28695. https://doi.org/10.1038/srep28695.

(22) Huš, S.; Krajnc, P. PolyHIPEs from Methyl Methacrylate: Hierarchically Structured Microcellular Polymers with Exceptional Mechanical Properties. *Polymer (Guildf).* **2014**, *55* (17), 4420–4424. https://doi.org/10.1016/j.polymer.2014.07.007.

(23) Aldemir Dikici, B.; Sherborne, C.; Reilly, G. C.; Claeyssens, F. Emulsion Templated Scaffolds Manufactured from Photocurable Polycaprolactone. *Polymer (Guildf).* **2019**, *175* (2019), 243–254. https://doi.org/10.1016/j.polymer.2019.05.023.

(24) Aldemir Dikici, B.; Dikici, S.; Reilly, G. C.; MacNeil, S.; Claeyssens, F. A Novel Bilayer Polycaprolactone Membrane for Guided Bone Regeneration: Combining Electrospinning and Emulsion Templating. *Materials (Basel).* **2019**, *12* (16), 2643. https://doi.org/10.3390/ma12162643.

(25) Wang, A.; Paterson, T.; Owen, R.; Sherborne, C.; Dugan, J.; Li, J.; Claeyssens, F. Photocurable High Internal Phase Emulsions (HIPEs) Containing Hydroxyapatite for Additive Manufacture of Tissue Engineering Scaffolds with Multi-Scale Porosity. *Mater. Sci. Eng. C* **2016**, *67* (2016), 51–58. https://doi.org/10.1016/j.msec.2016.04.087.

(26) Caldwell, S.; Johnson, D. W.; Didsbury, M. P.; Murray, B. A.; Wu, J. J.; Przyborski, S. A.; Cameron, N. R. Degradable Emulsion-Templated Scaffolds for Tissue Engineering from Thiol-Ene Photopolymerisation. *Soft Matter* **2012**, *8* (40), 10344–10351. https://doi.org/10.1039/c2sm26250a.

(27) Kimmins, S. D.; Wyman, P.; Cameron, N. R. Photopolymerised Methacrylate-Based Emulsion-Templated Porous Polymers. *React. Funct. Polym.* **2012**, *72* (12), 947–954. https://doi.org/10.1016/j.reactfunctpolym.2012.06.015.

(28) Sears, N. A.; Dhavalikar, P. S.; Cosgriff-Hernandez, E. M. Emulsion Inks for 3D Printing of High Porosity Materials. *Macromol. Rapid Commun.* **2016**, *37* (16), 1369–1374. https://doi.org/10.1002/marc.201600236.

(29) Lovelady, E.; Kimmins, S. D.; Wu, J.; Cameron, N. R. Preparation of Emulsion-Templated Porous Polymers Using Thiol-Ene and Thiol-Yne Chemistry. *Polym. Chem.* **2011**, *2* (3), 559–562. https://doi.org/10.1039/c0py00374c.

(30) Johnson, D. W.; Langford, C. R.; Didsbury, M. P.; Lipp, B.; Przyborski, S. A.; Cameron, N. R. Fully Biodegradable and Biocompatible Emulsion Templated Polymer Scaffolds by Thiol-Acrylate Polymerization of Polycaprolactone Macromonomers. *Polym. Chem.* **2015**, *6* (41), 7256–7263. https://doi.org/10.1039/c5py00721f.

(31) Sušec, M.; Liska, R.; Russmüller, G.; Kotek, J.; Krajnc, P. Microcellular Open Porous Monoliths for Cell Growth by Thiol-Ene Polymerization of Low-Toxicity Monomers in High Internal Phase Emulsions. *Macromol. Biosci.* **2015**, *15* (2), 253–261. https://doi.org/10.1002/mabi.201400219.

(32) Whitely, M. E.; Robinson, J. L.; Stuebben, M. C.; Pearce, H. A.; McEnery, M. A. P.; Cosgriff-Hernandez, E. Prevention of Oxygen Inhibition of PolyHIPE Radical Polymerization Using a Thiol-Based Cross-Linker. *ACS Biomater. Sci. Eng.* **2017**, *3* (3), 409–419. https://doi.org/10.1021/acsbiomaterials.6b00663.

(33) Langford, C. R.; Johnson, D. W.; Cameron, N. R. Chemical Functionalization of Emulsion-Templated Porous Polymers by Thiol-Ene "Click" Chemistry. *Polym. Chem.* **2014**, *5* (21), 6200–6206. https://doi.org/10.1039/c4py00713a.

(34) da Silva, M. A.; Crawford, A.; Mundy, J.; Martins, A.; Araújo, J. V.; Hatton, P. V.; Reis, R. L.; Neves, N. M. Evaluation of Extracellular Matrix Formation in Polycaprolactone and Starch-Compounded Polycaprolactone Nanofiber Meshes When Seeded with Bovine Articular Chondrocytes. *Tissue Eng. Part A* **2009**, *15* (2), 377–385. https://doi.org/10.1089/ten.tea.2007.0327.

(35) Dikici, S.; Claeyssens, F.; MacNeil, S. Pre-Seeding of Simple Electrospun Scaffolds with a Combination of Endothelial Cells and Fibroblasts Strongly Promotes Angiogenesis. *Tissue Eng. Regen. Med.* **2020**, *17* (4), 445–458. https://doi.org/10.1007/s13770-020-00263-7.

(36) Dikici, S.; Aldemir Dikici, B.; MacNeil, S.; Claeyssens, F. Decellularised Extracellular Matrix Decorated PCL PolyHIPE Scaffolds for Enhanced Cellular Activity, Integration and Angiogenesis. *Biomater. Sci.* **2021**, Just accepted. https://doi.org/10.1039/D1BM01262B.

(37) Aldemir Dikici, B. Development of Emulsion Templated Matrices and Their Use in Tissue Engineering Applications, The University of Sheffield, 2020.

(38) Dikici, S.; Mangır, N.; Claeyssens, F.; Yar, M.; MacNeil, S. Exploration of 2-Deoxy-D-Ribose and 17β-Estradiol as Alternatives to Exogenous VEGF to Promote Angiogenesis in Tissue-Engineered Constructs. *Regen. Med.* **2019**, *14* (3), 179–197. https://doi.org/10.2217/rme-2018-0068.

(39) Carnachan, R. J.; Bokhari, M.; Przyborski, S. A.; Cameron, N. R. Tailoring the Morphology of Emulsion-Templated Porous Polymers. *Soft Matter* **2006**, *2* (7), 608. https://doi.org/10.1039/b603211g.

(40) Huš, S.; Kolar, M.; Krajnc, P. Tailoring Morphological Features of Cross-Linked Emulsion-Templated Poly(Glycidyl Methacrylate). *Des. Monomers Polym.* **2015**, *18* (7), 698–703. https://doi.org/10.1080/15685551.2015.1070503.

(41) Dikici, S.; Claeyssens, F.; MacNeil, S. Decellularised Baby Spinach Leaves and Their Potential Use in Tissue Engineering Applications: Studying and Promoting Neovascularisation. *J. Biomater. Appl.* **2019**, *0* (0), 1–14. https://doi.org/10.1177/0885328219863115.

(42) Dikici, S.; Bullock, A. J.; Yar, M.; Claeyssens, F.; MacNeil, S. 2-Deoxy-d-Ribose (2dDR) Upregulates Vascular Endothelial Growth Factor (VEGF) and Stimulates Angiogenesis. *Microvasc. Res.* **2020**, *131*, 104035. https://doi.org/10.1016/j.mvr.2020.104035.

(43) Bak, T. Y.; Kook, M. S.; Jung, S. C.; Kim, B. H. Biological Effect of Gas Plasma Treatment on CO2 Gas Foaming/Salt Leaching Fabricated Porous Polycaprolactone Scaffolds in Bone Tissue Engineering. *J. Nanomater.* **2014**, *2014*, 1–6. https://doi.org/10.1155/2014/657542.

(44) Reignier, J.; Huneault, M. A. Preparation of Interconnected Poly(E{lunate}-Caprolactone) Porous Scaffolds by a Combination of Polymer and Salt Particulate Leaching. *Polymer (Guildf).* **2006**, *47* (13), 4703–4717. https://doi.org/10.1016/j.polymer.2006.04.029.

(45) Elomaa, L.; Teixeira, S.; Hakala, R.; Korhonen, H.; Grijpma, D. W.; Seppälä, J. V. Preparation of Poly(ε-

Caprolactone)-Based Tissue Engineering Scaffolds by Stereolithography. *Acta Biomater.* **2011**, *7* (11), 3850–3856. https://doi.org/10.1016/j.actbio.2011.06.039.

(46) Singh, D.; Harding, A. J.; Albadawi, E.; Boissonade, F. M.; Haycock, J. W.; Claeyssens, F. Additive Manufactured Biodegradable Poly(Glycerol Sebacate Methacrylate) Nerve Guidance Conduits. *Acta Biomater.* **2018**, *78* (2018), 48–63. https://doi.org/10.1016/j.actbio.2018.07.055.

(47) Pashneh-Tala, S.; Owen, R.; Bahmaee, H.; Rekštytė, S.; Malinauskas, M.; Claeyssens, F. Synthesis, Characterization and 3D Micro-Structuring via 2-Photon Polymerization of Poly(Glycerol Sebacate)-Methacrylate–An Elastomeric Degradable Polymer. *Front. Phys.* **2018**, *6* (41), 1–17. https://doi.org/10.3389/fphy.2018.00041.

(48) Pashneh-Tala, S.; Moorehead, R.; Claeyssens, F. Hybrid Manufacturing Strategies for Tissue Engineering Scaffolds Using Methacrylate Functionalised Poly(Glycerol Sebacate). *J. Biomater. Appl.* **2020**, *34* (8), 1114–1130. https://doi.org/10.1177/0885328219898385.

(49) Busby, W.; Cameron, N. R.; Jahoda, C. A. B. Tissue Engineering Matrixes by Emulsion Templating. *Polym. Int.* **2002**, *51* (10), 871–881. https://doi.org/10.1002/pi.934.

(50) Busby, W.; Cameron, N. R.; Jahoda, C. A. B. Emulsion-Derived Foams (PolyHIPEs) Containing Poly(Sε-Caprolactone) as Matrixes for Tissue Engineering. *Biomacromolecules* **2001**, *2* (1), 154–164. https://doi.org/10.1021/bm0000889.

(51) Moglia, R. S.; Robinson, J. L.; Muschenborn, A. D.; Touchet, T. J.; Maitland, D. J.; Cosgriff-Hernandez, E. Injectable PolyMIPE Scaffolds for Soft Tissue Regeneration. *Polymer (Guildf).* **2014**, *55* (1), 426–434. https://doi.org/10.1016/j.polymer.2013.09.009.

(52) Diez-Ahedo, R.; Mendibil, X.; Márquez-Posadas, M. C.; Quintana, I.; González, F.; Rodríguez, F. J.; Zilic, L.; Sherborne, C.; Glen, A.; Taylor, C. S.; et al. UV-Casting on Methacrylated PCL for the Production of a Peripheral Nerve Implant Containing an Array of Porous Aligned Microchannels. *Polymers (Basel).* **2020**, *12* (4), 971. https://doi.org/10.3390/polym12040971.

(53) Green, B. J.; Worthington, K. S.; Thompson, J. R.; Bunn, S. J.; Rethwisch, M.; Kaalberg, E. E.; Jiao, C.; Wiley, L. A.; Mullins, R. F.; Stone, E. M.; et al. Effect of Molecular Weight and Functionality on Acrylated Poly(Caprolactone) for Stereolithography and Biomedical Applications. *Biomacromolecules* **2018**, *19* (9), 3682–3692. https://doi.org/10.1021/acs.biomac.8b00784.

(54) Woodruff, M. A.; Hutmacher, D. W. The Return of a Forgotten Polymer - Polycaprolactone in the 21st Century. *Prog. Polym. Sci.* **2010**, *35* (10), 1217–1256. https://doi.org/10.1016/j.progpolymsci.2010.04.002.

(55) Busby, W.; Cameron, N. R.; Jahoda, C. A. B. Emulsion-Derived Foams (PolyHIPEs) Containing Poly(ε-Caprolactone) as Matrixes for Tissue Engineering. *Biomacromolecules* **2001**, *2* (1), 154–164. https://doi.org/10.1021/bm0000889.

(56) Lumelsky, Y.; Lalush-Michael, I.; Levenberg, S.; Silverstein, M. S. A Degradable, Porous, Emulsion-Templated Polyacrylate. *J. Polym. Sci. Part A Polym. Chem.* **2009**, *47* (24), 7043–7053. https://doi.org/10.1002/pola.23744.

(57) Lumelsky, Y.; Silverstein, M. S. Biodegradable Porous Polymers through Emulsion Templating. *Macromolecules* **2009**, *42* (5), 1627–1633. https://doi.org/10.1021/ma802461m.

(58) Pérez-García, M. G.; Gutiérrez, M. C.; Mota-Morales, J. D.; Luna-Bárcenas, G.; Del Monte, F. Synthesis of Biodegradable Macroporous Poly(l -Lactide)/Poly(ϵ-Caprolactone) Blend Using Oil-in-Eutectic-Mixture High-Internal-Phase Emulsions as Template. *ACS Appl. Mater. Interfaces* **2016**, *8* (26), 16939–16949. https://doi.org/10.1021/acsami.6b04830.

(59) Yang, X.; Yin, Z.; Zhang, X.; Zhu, Y.; Zhang, S. Fabrication of Emulsion-Templated Macroporous Poly(ε-Caprolactone) towards Highly Effective and Sustainable Oil/Water Separation. *Polymer (Guildf).* **2020**, *204*. https://doi.org/10.1016/j.polymer.2020.122852.

(60) Yadav, A.; Pal, J.; Nandan, B.; Srivastava, R. K. Macroporous Scaffolds of Cross-Linked Poly(ε-Caprolactone)via High Internal Phase Emulsion Templating. *Polymer (Guildf).* **2019**, *176*, 66–73. https://doi.org/10.1016/j.polymer.2019.05.034.

(61) David, D.; Silverstein, M. S. Porous Polyurethanes Synthesized within High Internal Phase Emulsions. *J. Polym. Sci. Part A Polym. Chem.* **2009**, *47* (21), 5806–5814. https://doi.org/10.1002/pola.23624.

(62) Changotade, S.; Radu Bostan, G.; Consalus, A.; Poirier, F.; Peltzer, J.; Lataillade, J. J.; Lutomski, D.; Rohman, G. Preliminary in Vitro Assessment of Stem Cell Compatibility with Cross-Linked Poly(ε -Caprolactone Urethane) Scaffolds Designed through High Internal Phase Emulsions. *Stem Cells Int.* **2015**. https://doi.org/10.1155/2015/283796.

(63) Field, J.; Haycock, J. W.; Boissonade, F. M.; Claeyssens, F. A Tuneable, Photocurable, Poly(Caprolactone)-Based Resin for Tissue Engineering—Synthesis, Characterisation and Use in Stereolithography. *Molecules* **2021**, *26* (5), 1199. https://doi.org/10.3390/molecules26051199.

(64) Han, S. B.; Kim, J. K.; Lee, G.; Kim, D. H. Mechanical Properties of Materials for Stem Cell Differentiation. *Adv. Biosyst.* **2020**, *4* (11). https://doi.org/10.1002/adbi.202000247.

(65) Hah, J.; Kim, D.-H. Deciphering Nuclear Mechanobiology in Laminopathy. *Cells* **2019**, *8* (3). https://doi.org/10.3390/cells8030231.

(66) Narasimhan, B. N.; Ting, M. S.; Kollmetz, T.; Horrocks, M. S.; Chalard, A. E.; Malmström, J. Mechanical Characterization for Cellular Mechanobiology: Current Trends and Future Prospects. *Frontiers in Bioengineering and Biotechnology*. 2020. https://doi.org/10.3389/fbioe.2020.595978.

(67) Kida, T.; Tanaka, R.; Nitta, K. H.; Shiono, T. Effect of the Number of Arms on the Mechanical Properties of a Star-Shaped Cyclic Olefin Copolymer. *Polym. Chem.* **2019**, *10* (41). https://doi.org/10.1039/c9py01186b.

(68) Doganci, M. D. Effects of Star-Shaped PCL Having Different Numbers of Arms on the Mechanical, Morphological, and Thermal Properties of PLA/PCL Blends. *J. Polym. Res.* **2021**, *28* (1). https://doi.org/10.1007/s10965-020-02380-2.

(69) Wang, S.; Kempen, D. H.; Simha, N. K.; Lewis, J. L.; Windebank, A. J.; Yaszemski, M. J.; Lu, L. Photo-Cross-Linked Hybrid Polymer Networks Consisting of Poly(Propylene Fumarate) and Poly(Caprolactone Fumarate): Controlled Physical Properties and Regulated Bone and Nerve Cell Responses. *Biomacromolecules* **2008**. https://doi.org/10.1021/bm7012313.

(70) Tian, G.; Zhu, G.; Ren, T.; Liu, Y.; Wei, K.; Liu, Y. X. The Effects of PCL Diol Molecular Weight on Properties of Shape Memory Poly(ε-Caprolactone) Networks. *J. Appl. Polym. Sci.* **2019**, *136* (6). https://doi.org/10.1002/app.47055.

(71) Peponi, L.; Navarro-Baena, I.; Báez, J. E.; Kenny, J. M.; Marcos-Fernández, A. Effect of the Molecular Weight on the Crystallinity of PCL-b-PLLA Di-Block Copolymers. *Polymer (Guildf).* **2012**, *53* (21). https://doi.org/10.1016/j.polymer.2012.07.066.

(72) Wang, S.; Yaszemski, M. J.; Gruetzmacher, J. A.; Lu, L. Photo-Crosslinked Poly(ε-Caprolactone Fumarate) Networks: Roles of Crystallinity and Crosslinking Density in Determining Mechanical Properties. *Polymer (Guildf).* **2008**, *49* (26). https://doi.org/10.1016/j.polymer.2008.10.021.

(73) Paterson, T. E.; Gigliobianco, G.; Sherborne, C.; Green, N. H.; Dugan, J. M.; MacNeil, S.; Reilly, G. C.;

637 Claeyssens, F. Porous Microspheres Support Mesenchymal Progenitor Cell Ingrowth and Stimulate
638 Angiogenesis. *APL Bioeng.* **2018**, *2* (2), 026103. https://doi.org/10.1063/1.5008556.

639 (74) Moglia, R. S.; Holm, J. L.; Sears, N. A.; Wilson, C. J.; Harrison, D. M.; Cosgriff-Hernandez, E. Injectable
640 PolyHIPEs as High-Porosity Bone Grafts. *Biomacromolecules* **2011**, *12* (10), 3621–3628.
641 https://doi.org/10.1021/bm2008839.

642 (75) Grosvenor, M. P.; Staniforth, J. N. The Effect of Molecular Weight on the Rheological and Tensile
643 Properties of Poly(ε-Caprolactone). *Int. J. Pharm.* **1996**, *135* (1–2). https://doi.org/10.1016/0378-
644 5173(95)04404-3.

645 (76) Aslantürk, Ö. S. In Vitro Cytotoxicity and Cell Viability Assays: Principles, Advantages, and Disadvantages.
646 In *Genotoxicity - A Predictable Risk to Our Actual World*; InTech, 2018.
647 https://doi.org/10.5772/intechopen.71923.

648

649

650 ***For Table of Contents Only***

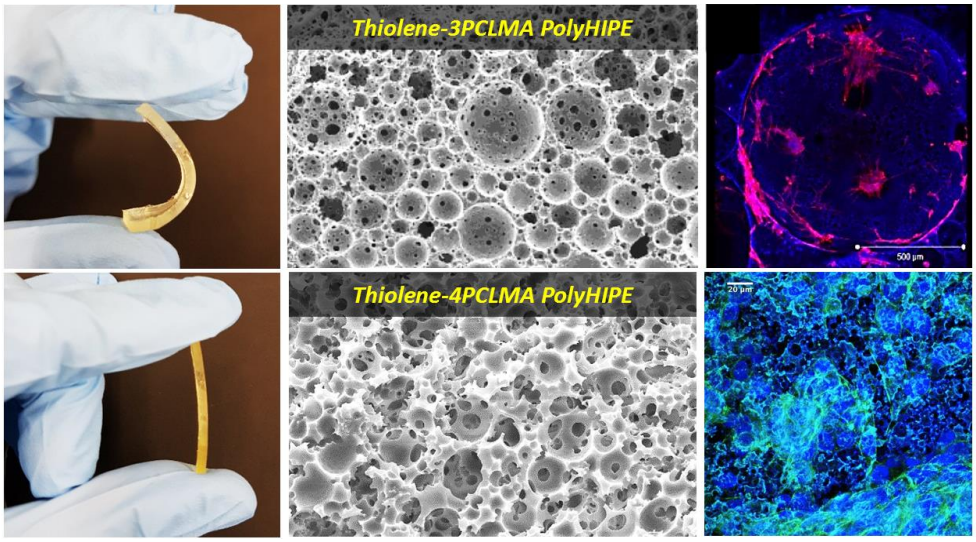

651